Process Safety and Environmental Protection 125 (2019) 164–171

Contents lists available at ScienceDirect

Process Safety and Environmental Protection

journal homepage: www.elsevier.com/locate/psep

Multiscale modeling of shock wave propagation induced by coal and gas outbursts

Aitao Zhou [a,b,c], Lingpeng Fan [a], Kai Wang [a,*], Derek Elsworth [c]

[a] School of Resource and Safety Engineering, China University of Mining and Technology (Beijing), Beijing, 100083, China
[b] State and Local Joint Engineering Laboratory for Gas Drainage & Ground Control of Deep Mines, Henan Polytechnic University, Jiaozuo, 454003, China
[c] Department of Energy and Mineral Engineering, EMS Energy Institute and G3 Center, Pennsylvania State University, University Park, PA, USA

ARTICLE INFO

Article history:
Received 13 November 2018
Received in revised form 29 January 2019
Accepted 22 February 2019
Available online 15 March 2019

Keywords:
Coal and gas outburst
Shock wave propagation
Multiscale coupling
Flowmaster
MPCCI coupling

ABSTRACT

We explore the propagation modes of shock waves driven by coal and gas outbursts in both the near- and far-field. Near-field response is three-dimensional (3D) at the face, but the far-field is constrained to one-dimensional (1D) flow within the roadways. Fluent models are applied to simulate the 3D propagation of shock waves at the outburst source with 1D models utilizing Flowmaster being sufficient distal from the face. These models are linked via a Mesh-based parallel Code Coupling Interface (MPCCI) to define shock wave propagation at all scales – from mine face to distal roadways. The results demonstrate the suitability and fidelity of the Flowmaster 1D simulation in representing the time history of overpressure. The shock wave attenuation in each part of the MPCCI coupled model is consistent with experimental results. This work provides a logical, consistent and robust method to solve for the complex coupling at multiple length- and time-scales and its implementation as an "outburst" pipe network. Additionally, it has significant utility in designing for outburst mitigation, disaster ventilation and other safety measures.

Contents

1. Introduction

With the increased demand for energy and the depletion of near surface resources, mining probes progressively to greater depths (Liu et al., 2014, 2016; Zhang et al., 2016; Wang et al., 2017). Increasing ground stresses at depth both reduce permeability and increase sorptive gas storage, elevating the potential for coal and gas outbursts during mining (Wang et al., 2014a, b; Xu et al., 2016; Zhou et al., 2017a, b). The intensity and frequency of coal and gas outbursts are correspondingly increased, elevating the related hazard (Han et al., 2012; Hu et al., 2012; Guo et al., 2016; Tang et al., 2016). Intense high overpressure transient shock waves may result from such outbursts and disrupt underground production and damage and harm personnel, production facilities and the ventilation network. Therefore, it is important to understand the propagation characteristics of the outburst shock wave for design of outburst prevention facilities, to guide the form of the ventilation system and to reduce the outburst hazard. At present, due to the typically

* Corresponding author.
E-mail address: safety226@126.com (K. Wang).

https://doi.org/10.1016/j.psep.2019.02.026
0957-5820/

full destruction resulting from hazardous outbursts, few forensic details survive to allow the recovery of key features of causality and propagation. Thus, modeling is a useful tool to match sparse observations of the dynamic pressure response and thereby analyze and constrain causative mechanisms and propose mitigative methods.

Constraining measurements are typically limited to the post-failure architecture of the outburst site and records of propagation of the pressure pulse. One such in situ measurement is available for an outburst at a coal mine in the Zhongliang Mountains in 1977 where the static head generated by the gas and pulverized coal flow is of the order 0.3 - 0.6 MPa - representing a strong dynamic shock and destructive force. The causal mechanism of the outburst shock wave was analyzed and an attenuation formula deduced (Zhou et al., 2014, 2015). A physical model of outburst formation was proposed and numerically simulated, including the outburst process and development of the shock wave. These included the analysis of the influence of coal seam gas pressure and outburst intensity on the shock dynamic attenuation (Wang et al., 2012; Zhou et al., 2014). However, the research scope of this prior work was confined solely to consideration of the dynamic shock response in the surrounding roadway (near-field). The propagation of the outburst shock wave in the branches of the roadway was neglected. The dynamic shock force generated by the outburst is strong, so a significant dynamic force prevails in the roadway to considerable distance from the outburst source (Cheng and Yang, 2012; Nowak and Piątek, 2014; Zapletal et al., 2014; Kazakov et al., 2015; Kursunoglu and Onder, 2015; Wei et al., 2015). This current study explores the characteristics of shock wave propagation in the roadway surrounding the outburst source to define modes of propagation to distal areas in the mine. We adopt a one-dimensional simplified model to simulate the propagation of the shock wave in the roadway far from outburst source, scaling this to a 3D model in the face. The shock wave propagation model for the entire roadway network is then established by means of the MPCCI coupling method. The advantages are as follows: the propagation and attenuation of outburst shock wave in near-field of the outburst source are very complicate, only three-dimensional (3D) can represent the propagation law accurately. However, in far-field of the outburst source, most of the outburst shock wave attenuates only along the axial direction, to save calculations, one-dimensional (1D) model is best choice.

2. Theoretical analysis of flowmaster one-dimensional model

We use an equivalent 1D model to represent flow in individual roadways that accommodates mass and momentum transfer. This dynamic model is linked to the anticipated true 3D propagation of the outburst from the face.

2.1. One-dimensional simplicity principle

As the outburst shock wave propagates from the outburst source, turbulent effects are gradually muted and the pulverized coal will progressively settle along the roadway. The fluid parameter and the gradient of the impact airflow is mainly reflected in the propagation direction. The impacts of overpressure are highly variable in the direction of the airflow and rather uniform in the transverse direction. Thus, transport along the cross-section of the roadway can be simplified as a 1D airflow, so that a two-dimensional simulation in FLUENT, representing the outburst face, can be represented by 1D treatment in Flowmaster. This has a significant effect on computational efficiency and in reducing numerical calculation times. The high-speed compressed airflow is a transient compressible and non-viscous one-dimensional flow. The mass, momentum and energy conservation expression for this 1D representation in the pipeline network system is,

$$\begin{aligned}
&\frac{\partial p}{\partial t}+V\frac{\partial V}{\partial x}+\rho a^2\frac{\partial V}{\partial x}=\frac{a^2}{C_pT}\left[1+\frac{T}{Z}\left(\frac{\partial Z}{\partial T}\right)T\right]\frac{\Omega+WV}{A}\\
&\frac{\partial V}{\partial t}+V\frac{\partial V}{\partial x}+\frac{1}{\rho}\frac{\partial p}{\partial x}=\frac{W}{A\rho}-g\sin\theta\\
&\frac{\partial T}{\partial t}+V\frac{\partial T}{\partial x}+\frac{a^2}{C_p}\left[1+\frac{T}{Z}\left(\frac{\partial Z}{\partial T}\right)p\right]\frac{\partial V}{\partial x}\\
&\quad=\frac{a^2}{C_pp}\left[1-\frac{P}{Z}\left(\frac{\partial Z}{\partial p}\right)T\right]\frac{\Omega+WV}{A}\\
&W=f\frac{A}{D}\rho\frac{V|V|}{2}
\end{aligned}\tag{1}$$

where V is velocity, m/s; x is the axis distance, m; a is the sound speed, m/s; Cp is specific heat, $J/(kg\cdot K)$; Z is the compressibility coefficient of gas; A is the flow area, m^2; Ω is the unit length heat consumption, J/m; g is a gravitational acceleration, m/s^2; θ is the inclination angle of the flow conduit from the horizontal; W is frictional energy loss, J; and f is the Darcy friction factor, dimensionless; In practice, the propagation of the shock wave is considered adiabatic and Ω can be neglected.

2.2. One-dimensional modeling assembly and pressure loss treatment

Flowmaster is a network modeling code capable of solving for mass, momentum and energy flows in complex pipe (line) networks. This model enables the simulation of the propagation of the outburst shock wave for gas flow in one-dimensional pipe networks with uniform transverse behavior representing an equivalent duct. The response relies on a rich library of network modeling elements, as follows:

(1) Source elements

Source elements define flow, pressure, heat and other boundary and initial conditions. The most commonly used elements in the mine ventilation model are pressure sources, flow sources and flow cut-off.

(2) Roadway geometric elements

Straight roadway: Gas flow within a circular tube may be used to represent outburst shock wave, where pressure loss is determined from the friction loss coefficient. The pressure drop is defined as,

$$P_2-P_1=\frac{fL}{d}\frac{\dot{m}_1|\dot{m}_1|}{2A^2\rho}\tag{2}$$

where, P_1 and P_2 are the pressure at inlet and outlet, respectively, MPa; f is the Darcy friction factor; L is the length of the tube, m; d is the tube diameter, m; and $\dot{m}_1$ is the mass flow rate at the inlet, kg/ s.

Diverging roadway: The diverging element accommodates different diverging angles. Attenuation of the pressure pulse is insignificant when the outburst shock wave propagates through the T-shaped branch. When the roadway diverges at only a small angle, the attenuation is found to be more severe than for a paralell T-junction. In Flowmaster, the equation representing pressure loss in the low-speed flow branch is:

$$\Delta p=\frac{C_{Re}k\dot{m}_c|\dot{m}_c|}{2\rho A_c}\tag{3}$$

C_{Re} is the modified Reynolds number; k is the branch loss coefficient; $\dot{m}_c$ is the mass flow rate at the branch inlet, kg/ s; A_c is the branch flow area, m^2. In the case of a high-speed outburst shock airflow, in Flowmaster, the additional pressure loss due to the change of geometric structure should also be taken into account. Therefore, as for the case of a small angle diverging roadway, the actual pressure loss of unilateral branch can be corrected as follows:

$$\Delta p = p_{t1}(1-\eta)/\eta \tag{4}$$

By modifying the front loss coefficient k, the equivalent effect can be obtained, and k is determined by the inlet pressure p_{t1} and the empirical attenuation coefficient η obtained through simulation, wherein p_{t1} is of the same order of magnitude as the overpressure of the roadway surrounding the outburst source.

Corner roadway: Corner roadways have significant influence on the propagation of shock airflow. Based on the attenuation coefficient η obtained through simulation, the corresponding pressure loss element C_d is used.

C_d pressure loss element achieves an equivalent effect in a way that defines the pressure loss. In Flowmaster, the specific control equation is:

$$\Delta p = \frac{8Lf}{\rho^2\pi d^5}\left(\frac{C_d A_t P_{t1}\Psi\sqrt{\frac{2}{R_s T_{t1} Z_1}}}{m_{t1}}\right)^2 \tag{5}$$

Here, m_{t1}, $P_{t1}$and T_{t1} are mass flow rate, the full pressure, and the upstream temperature of the discrete pressure loss element, respectively; f is the Darcy friction factor; Ψ is the flow function; Z_1 is the compressible coefficient of the upstream flow; and R_s is the gas constant. According to the pressure loss $\Delta p = p_{t1}(1-\eta)/\eta$, η is an empirical attenuation coefficient obtained through simulation. The equivalent attenuation effect can be achieved by setting the discrete loss coefficient C_d for a given η.

Variable cross-section roadway: In transitional element,s sudden enlargement and sudden contraction can be used to replace the change of roadway cross-section. Taking the case of sudden enlargement of roadway cross-section as an example, according to the Bernoulli equation, when the shock airflow decelerates into a suddenly enlarging cross-section, the airflow velocity decays, and the shock overpressure of the original cross-section instantaneously increases. In this state the kinetic energy is converted into an increased over-pressure According to the empirical attenuation coefficient η in FLUENT simulations, this structure has little effect on shock overpressure attenuation.

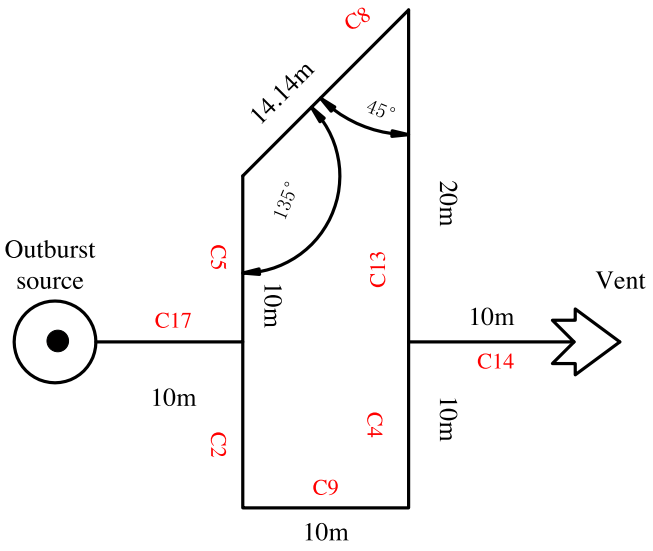

Fig. 1. Top view of the outburst roadways.

2.3. One-dimensional representation of far-field roadways

We propose a simple pipe network model using Flowmaster to simulate the migration of the shock wave. By adopting an equivalent outburst source, the characteristics are determined using a FLUENT two-dimensional simulation shock wave pressure attenuation data source. Given the pressure change P_1 (relative to atmospheric pressure), the ventilation element is simplified as a rigid circular section tube with a diameter of 2 m with an outlet at standard atmospheric pressure P_2 =0.1 MPa. A schematic of this roadway pipe network is shown in Fig. 1:

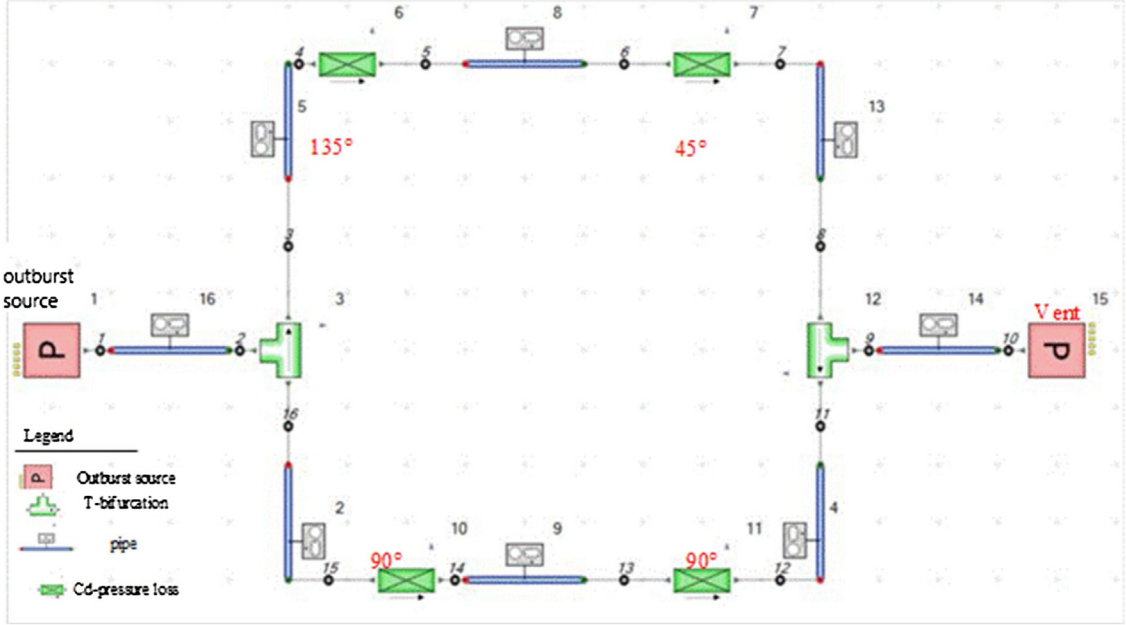

Fig. 2. Top view of outburst roadways based on Flowmaster simulations.

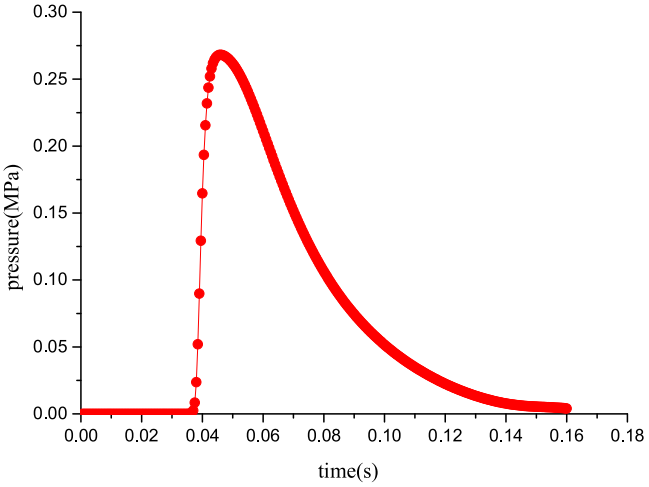

Fig. 3. Variation of shock airflow overpressure P_1 with time.

A model representing an outburst within a roadway pipe network for the Flowmaster code is shown in Fig. 2. The original pressures P_1 and P_{15} are adopted, respectively, to substitute the external atmospheric pressure environment connected with the outburst overpressure source and air outlet, respectively. At the four corners, simulation result from FLUENT define these as $\eta_{\theta=45^\circ} = 2.3$, $\eta_{\theta=90^\circ} = 1.7$,$\eta_{\theta=135^\circ} = 1.11$. The original pressure loss (C_d) is replaced, and an equivalent pressure loss is obtained according to equation (5). For the roadway T-shaped structure, the influence of the T-shaped structure itself is not significant, and the change in flow rate and pressure loss can be treated by adopting the T-shaped branch pipe.

FLUENT is used to represent the shock overpressure history in different roadway geometries to analyze the attenuation law and to tabulate the outburst shock wave. The outburst pressure source is imported into the corresponding overpressure attenuation characteristic curve in the Flowmaster model, and the simplified computation completed. The one-dimensional transient attenuation of the outburst shock wave is simulated, and the specific overpressure source characteristic curve is set as shown in Fig. 3:

The specific simulation results are shown in Fig. 4:

Fig. 4(a)–(h) shows the variation of shock pressure with respect to pipe length and time through pipes C2, C5, C8, C9, C4, C13, C14, and C16. The overpressure near the outburst source is 0.27 MPa. After the shock wave enters into the single network branches C5 and C8 through the T-shaped structure, the overpressure magnitude is 0.1 MPa, and when the shock overpressure propagates to branch C4, the peak value of overpressure attenuates to 0.045 MPa. This is within a reasonable range when it is compared with the simulation of the surrounding roadway of the outburst source; The entire propagation process is completed within 0.13 s, and the transitive hierarchy of pressure peak arrival times is recreated. Flowmaster is reliable for a one-dimensional simulation of the propagation of shock waves in network branches distant from outburst source.

The attenuation of overpressure is different for different roadway elements of equal length. Most of the conduits have an overpressure attenuation of 0.02 MPa within 10 m. In relation to that series-versus-parallel distribution, the position of the pipe is more important to the overpressure attenuation. For example, pipe C16 is close to the outburst pressure source - thus its attenuation amplitude is clear and the pressure peak is increased. As for pipe C14, which is located at the outlet and is close to atmospheric pressure, its peak pressure is not the same as for pipe C13 (which is distant from the outburst source) where the pressure peak is more obvious. It can be concluded that the pressure is greatly influenced by the form of the outlet.

Table 1
Verification of the attenuation effect of C_d pressure loss in the Flowmaster pipe network.

corner structure	Fluent attenuation coefficient η	FlowmasterC_d attenuation coefficient η
θ=45°	2.3	$\eta = \frac{P_8}{P_{13}} = 2.37$
θ=135°	1.11	$\eta = \frac{P_5}{P_8} = 1.10$
θ=90°	1.71	$\eta = \frac{P_2}{P_9} = 1.72$
θ=90°	1.71	$\eta = \frac{P_9}{P_4} = 1.56$

Table 1 lists a comparison between the Flowmaster pipe network model and equivalent pressure loss simulation for corner roadway shock wave attenuation coefficients relative to FLUENT simulation results. In Flowmaster, by adjusting the parameters of the pressure loss device C_d, the pressure loss is calculated in the reverse direction according to the attenuation coefficient η obtained from FLUENT. The attenuation effect, generated by adopting the pressure loss to replace the corner structure is consistent, and the method has considerable feasibility within a certain error range. Thus, the Flowmaster model is capable of representing one-dimensional dynamic flows.

3. Multiscale coupling of MPCCI software

3.1. Multiscale coupling

The Mesh-based Parallel Code Coupling Interface (MPCCI) is a standard computational outine to couple multi-physical fields in distributed parameter models. The coupling is based on its strong gridding self-adaptive ability, so that data transfer can be effected between one-dimensional and three-dimensional models. Thus, the two parameters of pressure and mass flow in a one-dimensional model (Flowmaster) may be routinely parsed to a three-dimensional model (FLUENT) for transient coupling, for example. The essence of the parameter exchange is to retain the flow and pressure of the one-dimensional nodes consistent with the total flow and surface pressure of the inlet and outlet units. FLUENT first sends the flow parameter to Flowmaster at the time of initialization of the transient exchange, performs parallel calculations, and then chooses to conduct regular exchange after each iterative step. In turn, FLUENT returns the flow parameters to Flowmaster and the iteration continues with exchange until convergence is reached.

3.2. Multiscale coupling for shock wave propagation

A simplified treatment is adopted in the MPCCI coupling between FLUENT-Flowmaster for shock wave propagation. The outburst source is simplified as a high-pressure cavity, and the outburst shock wave is only transmitted in one-direction (outbound) along the roadway. A 22 m long straight roadway with a height of 0.2 m is selected with an outburst cavity 0.5 m long and 0.3 m high (Fig. 5). The initial and boundary conditions for the FLUENT simulation in the near-field roadway are the original pressure of the outburst source, taken as the in situ gas pressure in coal seam. Compared to the outburst airflow, the actual normal gas concentration and gas flow velocity within the roadways are small and therefore neglected. Therefore, the initial air velocity in the outburst roadway is set as 0 m/s, the gas concentration set as null, and the initial pressure as atmospheric pressure.

The simulation of the surrounding roadway of the outburst source is processed by FLUENT and the coupling surface is arranged

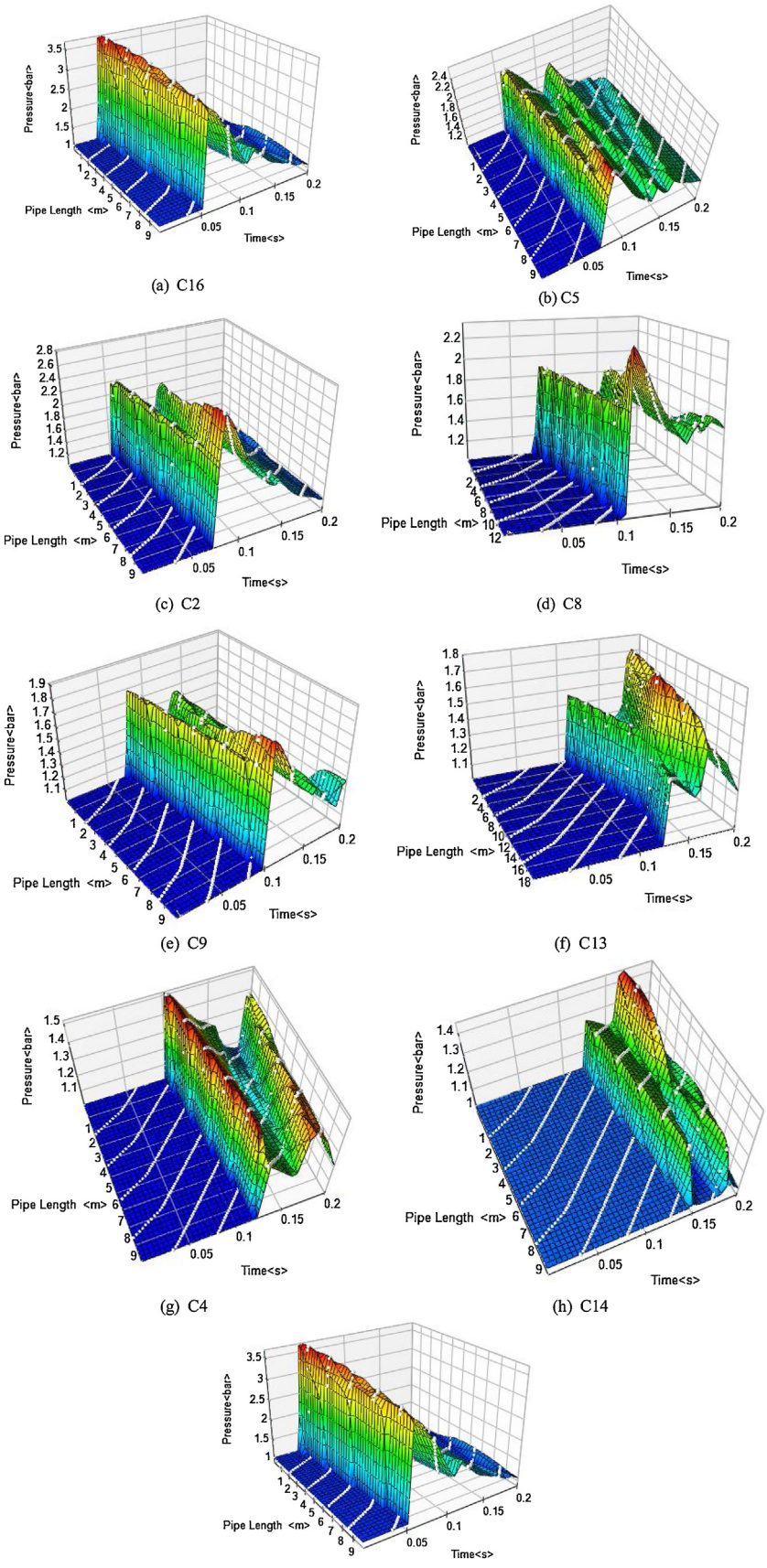

Fig. 4. Variation of outburst pressure with time and length along the network for different roadway forms.

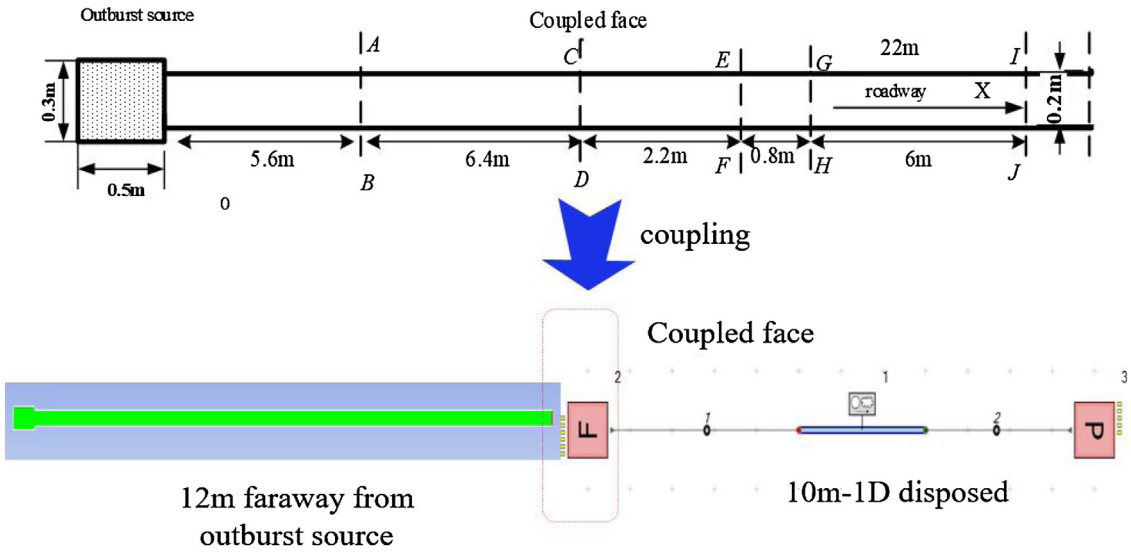

Fig. 5. Outburst coupling model for 22 m long straight roadway.

at a distance of 12 m from the outburst cavity. The overpressure attenuation gradient at this time is relatively small. The behavior in the 10 m roadway is subjected to one-dimensional linearization and the solution is then completed in Flowmaster.

In setting the coupling parameters, the flow source boundary is activated in Flowmaster, with an initial flow of 0.001 m^3/ s, and the transient compressible mode of simulation selected, with a time step of t = 0.0001 s, and a duration of simulation of 0.08 s; For FLUENT, the coupled face is set as the pressure outlet boundary. The coupling simulation adopts an explicit transient scheme, and Flowmaster is used as an initialization data receiver. The simulation results are shown in Fig. 6.

Fig. 6 shows the monitoring results of the coupled face CD at 12 m. The corresponding absolute pressure peak is 219418 Pa at t = 0.032 s, corresponding to an overpressure of 0.12 MPa, relative to atmospheric. This is consistent with the range of peak overpressures and their arrival time when separately simulated by FLUENT.

Comparison of the coupling around the outburst and the numerical simulation results from FLUENT are as shown in Fig. 7. The coupling simulation in FLUENT represents the front 12 m of the roadway adjacent to the outburst source acting along the 22 m roadway. At t = 0.01 s, the pressure in the outburst cavity is not completely released. At this time, the shock airflow has arrived at the

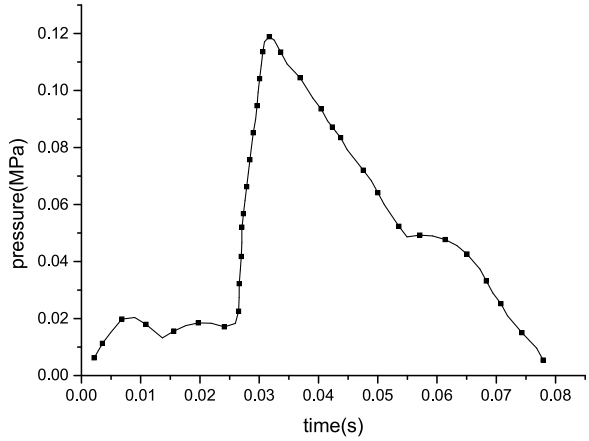

Fig. 6. Coupling face results. t=0.01 st=0.04 s. Shock airflow pressure/ MPaShock airflow pressure/ MPa.

2 m position in the roadway. At t = 0.04 s, the pressure in the outburst cavity has been completely released with an area of negative pressure close to the outlet when the peak pressure wave arrives at the 9 m position. At this time, the shock airflow has moved to the

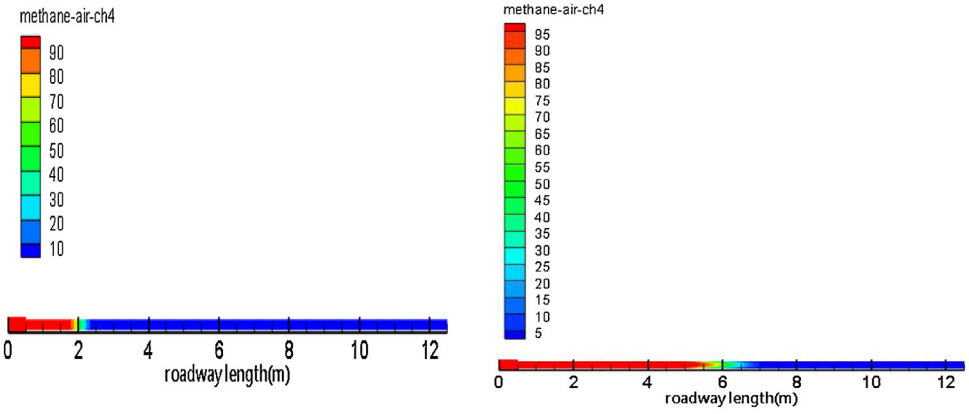

t=0.01s
Shock airflow pressure/ MPa

t=0.04s
Shock airflow pressure/ MPa

Fig. 7. Simulation results at different times in the area immediately surrounding the FLUENT outburst source. (a) 10 m long pipe absolute pressure varies with time and distance (b) Variation law of shock overpressure with time in different pipeline locations.

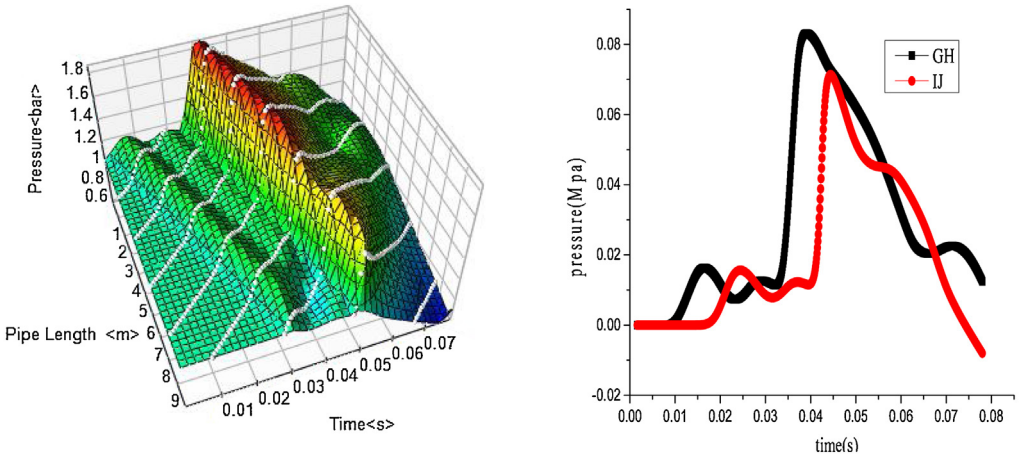

(a) 10 m long pipe absolute pressure varies with time and distance

(b) Variation law of shock overpressure with time in different pipeline locations

Fig. 8. Long distance simulation results from Flowmaster. (a) AB monitoring face (b) EF monitoring face.

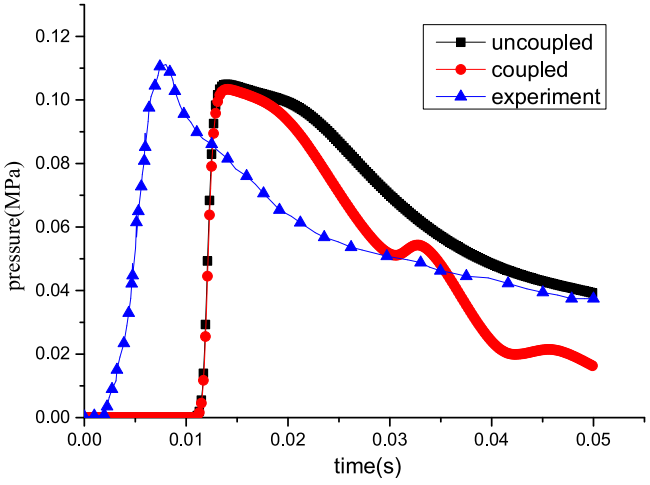

(a) AB monitoring face

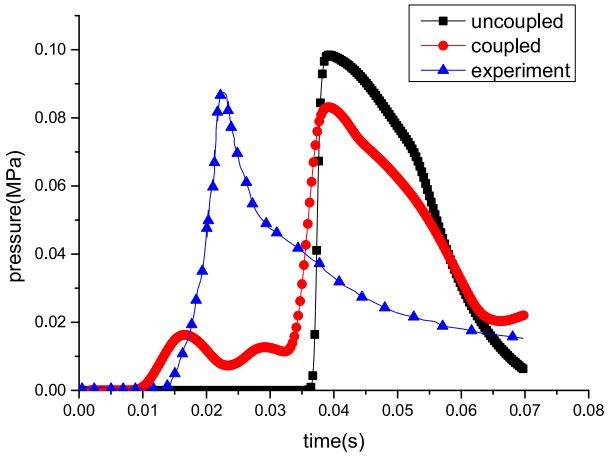

(b) EF monitoring face

Fig. 9. Shock wave overpressures with time for different roadway cross-sections.

6 m position, which is consistent with the rule separately simulated with FLUENT.

As shown in Fig. 8, a 10 m long network element located remotely from the outburst source is included in the coupling simulation. In the coupling process, the pressure source for Flowmaster is obtained by simulating using FLUENT at the 12 m location, and data transfer is performed by specifying the coupled face. Apparent from Fig. 8(a), pressure attenuation varies little along the flow domain with attenuation time. This is consistent with the individual simulation using Flowmaster; In Fig. 8(b), locations GH and IJ in the one-dimensional roadway are selected to verify the variation of overpressure with time. The arrival of peak overpressure at GH is extended to t = 0.037 s, and the overpressure peaks at 0.084 MPa, while the arrival at IJ is extended to t = 0.043 s at overpressure of 0.072Mpa.

As apparent in Fig. 9, the arrival of the simulated overpressure peak 5.6 m from the monitoring face at AB is Õ.012 s, while arrival in the experiment is at Õ.006 s. Despite this slight mismatch, the pressures in the simulation and experimental results are similar at Õ.11 MPa, while the trend between the three is similar at 14.2 m at the EF monitoring face. The pressure attenuation recorded in the simulation results is slower than in the experiments. This is mainly due to the pulverized coal used in the experiments settles quickly, while for the uniform particle flow adopted in the simulation process, the effect of gravity settling is not obvious. In addition, the peak pressure in the coupling simulation is slightly reduced over that of the non-coupling situation and the pressure attenuation is more rapid. This is mainly due to the influence of structure in the one-dimensional Flowmaster simulation being neglected. However, the experimental results are very close to the simulations and the trends in pressure response between the two methods is also consistent. In summary, multiscale coupling via MpCCI is highly reliable in the simulation of outburst shock wave propagation.

4. Conclusions

(1) Overpressures in roadways, generated by outbursts and shock airflows, vary significantly with time and attenuate only slightly along with the roadway. Conversely, the magnitude of the pressure change is highly sensitive to the outlet position.
(2) The Flowmaster-simulated peak pressure recorded in the shock wave distant from the outburst is reasonable and reliable. This reduced degree-of-freedom simulation is achieved by adopting

equivalent pressure loss elements to replace the true geometry of the roadway structure and the method is both effective and feasible.

(3) The treatment of attenuation of the shock wave of each part in the MPCCI multiscale coupling model is consistent with the experimental results – rendering the simulation model highly reliabile in the simulation of shock wave propagation.

Acknowledgments

This research is financially supported by National Natural Science Foundation of China (Grant No. 51774292, 51474219, 51604278), National Key R&D Program of China (2018YFC0808100), and the Open Funds of Hebei State Key Laboratory of Mine Disaster Prevention (Grant No. KJZH2017K02), the Yue Qi Distinguished Scholar Project, China University of Mining & Technology, Beijing, the Yue Qi Young Scholar Project, China University of Mining &Technology, Beijing, the Research Fund of State and Local Joint Engineering Laboratory for Gas Drainage & Ground Control of Deep Mines (Henan Polytechnic University).

References

Cheng, J., Yang, S., 2012. Data mining applications in evaluating mine ventilation system. Saf. Sci. 50 (4), 918–922.

Guo, H., et al., 2016. Pulverization characteristics of coal from a strong outburst-prone coal seam and their impact on gas desorption and diffusion properties. J. Nat. Gas Sci. Eng. 33, 867–878.

Han, J., et al., 2012. The characteristic of in situ stress in outburst area of China. Saf. Sci. 50 (4), 878–884.

Hu, Y., et al., 2012. Analysis on simulation experiment of outburst in uncovering coal seam in cross-cut. Procedia Eng. 45, 287–293.

Kazakov, B.P., et al., 2015. Stability of natural ventilation mode after main fan stoppage. Int. J. Heat Mass Transf. 86, 288–293.

Kursunoglu, N., Onder, M., 2015. Selection of an appropriate fan for an underground coal mine using the Analytic Hierarchy process. Tunn. Undergr. Space Technol. 48, 101–109.

Liu, Q., et al., 2014. A new effective method and new materials for high sealing performance of cross-measure CMM drainage boreholes. J. Nat. Gas Sci. Eng. 21, 805–813.

Liu, T., et al., 2016. Mechanical behaviors and failure processes of precracked specimens under uniaxial compression: a perspective from microscopic displacement patterns. Tectonophysics 672–673, 104–120.

Nowak, B., Piątek, J., 2014. verification of mathematical description of changes in air temperature and humidity in headings ventilated with auxiliary ventilation system/Weryfikacja Metematycznego Opisu Zmian Temperatury I Wilgotności Powietrza W Wyrobiskach Przewietrzanych Lutniciągiem Tłoczącym Z Dadatkowym Wentylatorem O Zmienianej Prędkości Obrotowej. Arch. Min. Sci. 59 (2).

Tang, J., et al., 2016. Line prediction technology for forecasting coal and gas outbursts during coal roadway tunneling. J. Nat. Gas Sci. Eng. 34, 412–418.

Wang, K., et al., 2012. Real-time numerical simulations and experimental research for the propagation characteristics of shock waves and gas flow during coal and gas outburst. Saf. Sci. 50 (4), 835–841.

Wang, G., et al., 2014a. Improved apparent permeability models of gas flow in coal with Klinkenberg effect. Fuel 128, 53–61.

Wang, K., et al., 2014b. Anisotropic permeability evolution of coal with effective stress variation and gas sorption: model development and analysis. Int. J. Coal Geol. 130, 53–65.

Wang, G., et al., 2017. Determining the diffusion coefficient of gas diffusion in coal: development of numerical solution. Fuel 196, 47–58.

Wei, X., et al., 2015. Multi-objective optimization of the HVAC (heating, ventilation, and air conditioning) system performance. Energy 83, 294–306.

Xu, C., et al., 2016. Square-form structure failure model of mining-affected hard rock strata: theoretical derivation, application and verification. Environ. Earth Sci. 75 (16).

Zapletal, P., et al., 2014. Effect of natural pressure drop in mine main ventilation/Skutki Naturalnego Spadku Ciśnienia W Głównej Sieci Wentylacyjnej Kopalni. Arch. Min. Sci. 59 (2).

Zhang, K., et al., 2016. Determination of sealing depth of in-seam boreholes for seam gas drainage based on drilling process of a drifter. Eng. Geol. 210, 115–123.

Zhou, A., et al., 2014. Propagation law of shock waves and gas flow in cross roadway caused by coal and gas outburst. Int. J. Min. Sci. Technol. 24 (1), 23–29.

Zhou, A., et al., 2015. Numerical simulation for propagation characteristics of shock wave and gas flow induced by outburst intensity. Int. J. Min. Sci. Technol. 25 (1), 107–112.

Zhou, A., et al., 2017a. Gas-solid coupling laws for deep high-gas coal seams. Int. J. Min. Sci. Technol. 27 (4), 675–679.

Zhou, A., et al., 2017b. A roadway driving technique for preventing coal and gas outbursts in deep coal mines. Environ. Earth Sci. 76 (6).